

Article

Natural Nitrogen Isotope Ratios as a Potential Indicator of N₂O Production Pathways in a Floodplain Fen

Mohit Masta ¹, Holar Sepp ², Jaan Pärn ¹, Kalle Kirsimäe ² and Ülo Mander ^{2,*}

¹ Department of Geography, Institute of Ecology and Earth Sciences, University of Tartu, Vanemuise 46, 51003 Tartu, Estonia; mohit.masta@ut.ee (M.M.); jaan.parn@ut.ee (J.P.)

² Department of Geology, University of Tartu, Institute of Ecology and Earth Sciences, Ravila 14a, 50411 Tartu, Estonia; holar.sepp@ut.ee (H.S.); kalle.kirsimae@ut.ee (K.K.)

* Correspondence: ulo.mander@ut.ee

Received: 30 December 2019; Accepted: 31 January 2020; Published: 4 February 2020



Abstract: Nitrous oxide (N₂O), a major greenhouse gas and ozone depleter, is emitted from drained organic soils typically developed in floodplains. We investigated the effect of the water table depth and soil oxygen (O₂) content on N₂O fluxes and their nitrogen isotope composition in a drained floodplain fen in Estonia. Measurements were done at natural water table depth, and we created a temporary anoxic environment by experimental flooding. From the suboxic peat (0.5–6 mg O₂/L) N₂O emissions peaked at 6 mg O₂/L and afterwards decreased with decreasing O₂. From the anoxic and oxic peat (0 and >6 mg O₂/L, respectively) N₂O emissions were low. Under anoxic conditions the δ¹⁵N/δ¹⁴N ratio of the top 10 cm peat layer was low, gradually decreasing to 30 cm. In the suboxic peat, δ¹⁵N/δ¹⁴N ratios increased with depth. In samples of peat fluctuating between suboxic and anoxic, the elevated ¹⁵N/¹⁴N ratios (δ¹⁵N = 7–9‰ ambient N₂) indicated intensive microbial processing of nitrogen. Low values of site preference (SP; difference between the central and peripheral ¹⁵N atoms) and δ¹⁸O-N₂O in the captured gas samples indicate nitrifier denitrification in the floodplain fen.

Keywords: anoxic; flooding experiment; nitrous oxide; natural abundance of ¹⁵N; oxygen; organic soil; suboxic

1. Introduction

Floodplains and other riparian ecosystems are important buffers controlling water quality and providing several other ecosystem services [1]. However, beside their water purification and habitat provision roles, riparian zones can be significant sources of greenhouse gas (GHG) emission [2]. Periodically flooded floodplains are a significant source of nitrous oxide (N₂O), a powerful GHG and a major ozone-depleting gas [3–5]. N₂O is produced in soil via nitrification under aerobic conditions, where ammonia is oxidized, and by denitrification, which occurs under anaerobic conditions, where nitrate is sequentially reduced to nitrite, NO, N₂O, and pure molecular nitrogen (N₂) [6]. The gaseous nitrogen losses directly depend on soil moisture, which affects oxygen availability in the soil. Hence, understanding the relationship between soil moisture, oxygen content, and N₂O emissions is highly important to understand N₂O production and consumption mechanisms in floodplains.

The effect of draining or flooding on nitrous oxide emissions has been studied in several studies. N₂O emissions follow a bell-shaped distribution with the peak at intermediate soil moisture [7]. Experiments show that variation in soil oxygen content induces high N₂O emissions [8]. Lower soil nitrate levels have been observed during the flooding periods, whereas a peak in N₂O emissions followed by a sudden drop has been observed as an after-effect of flooding [9]. These short-lived peaks, which were recorded when the water table was below soil surface, are also found to be a major source

of global N₂O emissions. When the soil was continuously and completely submerged, N₂O emissions dropped significantly [6,7,10,11].

For understanding the N₂O production, analysis of isotopic signatures has been developed in the past decades [12]. The N₂O molecule has an asymmetric structure (N-N-O) and the two N atoms are distinct referred to as beta (β) and alpha (α)-N^βN^αO [12]. It has also been shown that there is a preference for enrichment of ¹⁵N at the central (α) position of the N₂O molecule in atmosphere [13]. The ground state zero-point vibrational energy of ¹⁴N¹⁵N¹⁶O is less than ¹⁵N¹⁴N¹⁶O, which is why formation of the former is favoured over the latter under equilibrium conditions [14]. Also, the ¹⁴N-¹⁶O is reduced more easily as compared to ¹⁵N-¹⁶O, due to its low bond strength [15]. The enrichment of ¹⁵N at the central (α position) of the N₂O molecule has been observed during nitrification and denitrification [16,17]. Moreover, studies conducted with pure cultures of microbes producing N₂O have observed high site preferences (expressed as SP = δ¹⁵N^α – δ¹⁵N^β) for nitrification and low site preferences of ~0‰ for bacterial denitrification respectively [18–22]. High site preference has also been observed in fertilized arable soils indicating autotrophic nitrification [23]. Contrary to these results, there have also been studies that have shown non-uniform site preference during denitrification conditions, which creates a dilemma on answering the question of whether site preference can be used as a tool to differentiate between nitrification and denitrification [24–28].

The majority of ¹⁵N analyses related to N₂O fluxes have been made in mineral soils, and only a limited number of studies consider peat soils. For instance, Rückauf et al. (2004) [29] performed ¹⁵N tracer experiments in drained and reflooded microcosms filled with fen peat and found that denitrification was the main N transformation process, whereas N₂O emission from reflooded (anoxic) conditions was significantly lower than that from drained microcosms. Similar results were gained in field studies by Tauchnitz et al. (2015) [30] with ¹⁵N tracer studies on nitrogen gases released from a transition bog and found high N₂O and low N₂ from drained conditions and the reversed situation in rewetted cases. Likewise, Yang et al. (2011) [31] found significantly higher emission from drained soils with oxic conditions, using field-based ¹⁵N-N₂O pool dilution technique to measure gross N₂O production in soil. However, the natural isotope composition of N₂O to differentiate between nitrification and denitrification source processes has not been studied before in floodplain peats.

The objective of this study is to analyze the impact of water table depth and oxygen content on N₂O production pathways in a drained nitrogen-rich floodplain fen using experimental flooding and the natural isotope composition of N₂O.

2. Materials and Methods

2.1. Site Description

We collected gas samples from three positions in a drained fen in the floodplain of the Emajõgi River, Estonia (58°25′41.0″ N 26°30′30.3″ E; 58°25′38.2″ N 26°30′45.6″ E and 58°25′35.5″ N 26°31′02.8″ E) between 5 October and 12 November 2018. The positions differed in distance from the river, soil moisture, and oxygen concentration (Figure 1). We collected the gas samples from chambers to glass vials of 50 ml for gas analysis and 100ml for gas-isotope analysis. The chambers were organized in equilateral triangles. The side of the equilateral triangle was 1.6 meters. White 65-litre chambers were used on top of the collars to trap the gas emitted from the soil. Observation wells were placed to read the water table. The three positions were labelled as A, B, and C depending on their distance from the river. Position C was closest to the river and A was farthest away with B at the centre. During one-hour sessions, samples were collected after every 20 min and ten such sessions were conducted for this study. Position C was flooded with ditch water for 2 h before collecting samples using a garden pump to achieve anoxic conditions. Oxygen sensors (Fibox 4 by PreSens, Regensburg, Germany) were placed at depths of 5 cm, 25 cm, and 50 cm for a vertical oxygen profile at all three sampling positions. Soil temperature was monitored at all positions in each session at depths of 10 cm, 20 cm, 30 cm, and 40 cm. Soil samples were collected from at different depths.

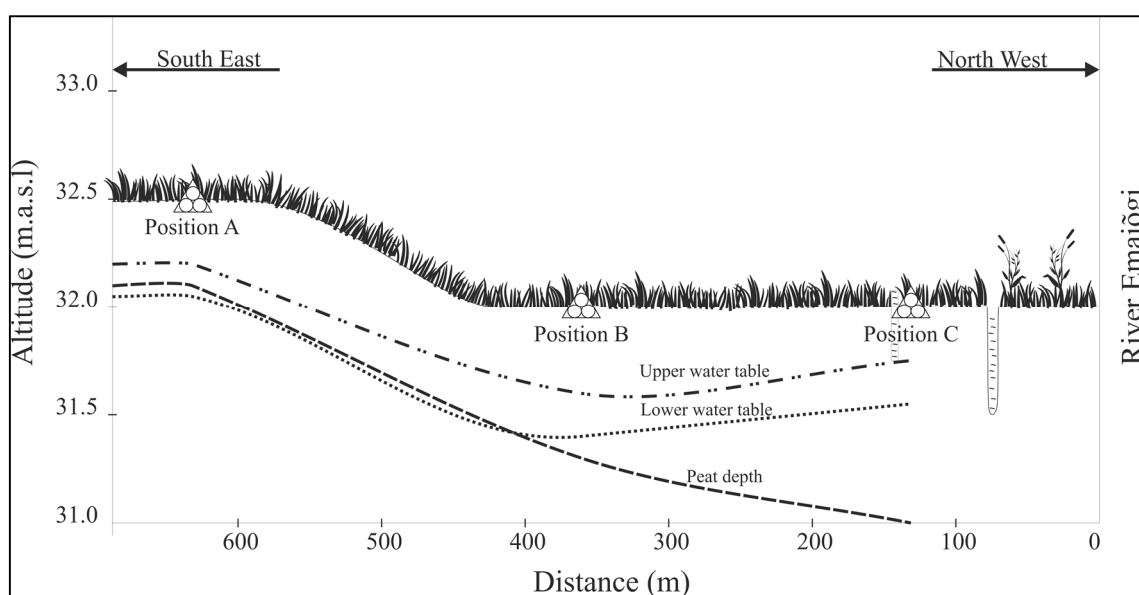


Figure 1. Study site view showing varying ground water level and peat depth at Kärevere in Tartu, Estonia.

2.2. Soil and Gas Isotope Analysis

Soil samples were collected at various depths. For bulk nitrogen isotope analysis, samples were dried to remove moisture and 1 milligram of each was packed into a tin capsule. Soil samples were then analyzed using a Delta V Plus mass spectrometer coupled with a Flash HT element analyser (Thermo Scientific, Bremen, Germany) in the Isotope Ratio Mass Spectrometer laboratory at University of Tartu. Nitrogen isotopes were calibrated against IAEA-N1 and IAEA-N2 international standards. Analytical precision was better than $\pm 0.2\text{‰}$. Soil chemical analysis was done at the Estonian University of Life Sciences. 100 mL of NH_4^+ —acetate solution was paired with titanium-yellow reagent. A flow injection analyser was used to determine plant-available magnesium (Mg^{2+}). To analyse available calcium (Ca^{2+}), the flame photometrical method was used with the same solution. Soil pH was calculated on a 1N KCl solution and flow-injection analysis was used on a 2M KCl extract of soil to determine soil $\text{NH}_4\text{-N}$ and $\text{NO}_3\text{-N}$. Oven-dried samples were used to determine total nitrogen via dry combustion method on a varioMAX CNS elemental analyzer (manufacturer: elementar, Langensfeld, Germany). Organic matter of oven-dry soil was calculated by loss on ignition at 360 °C . Soil bulk density was calculated considering that peat consists of organic matter, mineral matter, and water. Individual bulk densities of 0.23 , 2.65 , and 1 g/cm^3 for mineral matter, organic matter, and water, respectively, were used to calculate the bulk density of each peat sample [32,33].

Gas-phase N_2O concentrations were measured using a gas chromatograph equipped with an electron detector (GC-2014, Shimadzu, Kyoto, Japan). Soil gas N_2O isotopomer ratios (bulk nitrogen $\delta^{15}\text{N}_{\text{gas}}$), and ^{15}N site preference (SP) were concentrated and purified on a modified PreCon [34] and GasBench II and analyzed on a Delta V mass spectrometer (Thermo Scientific: Waltham, MA, USA) (Figure 2). We replaced the viton seals with rubber rings in PreCon and also bypassed the oven. We removed the sample loop in the GasBench II and used the same ports to connect PreCon, and used 100 ml sample bottles. For mass 31 measurements we used higher amplification (3.00×10^{11}) according to Potter et al. [35]. The isotope and site preference values were calculated according to Toyoda and Yoshida [12] and calibrated against standard reference gas.

Isotopomer ratios were noted as δ values defined as:

$$\delta^{15}\text{N}_i = R^{15}\text{sample}_i / R^{15}\text{standard} - 1 \quad (i = \alpha, \beta, \text{ or bulk})$$

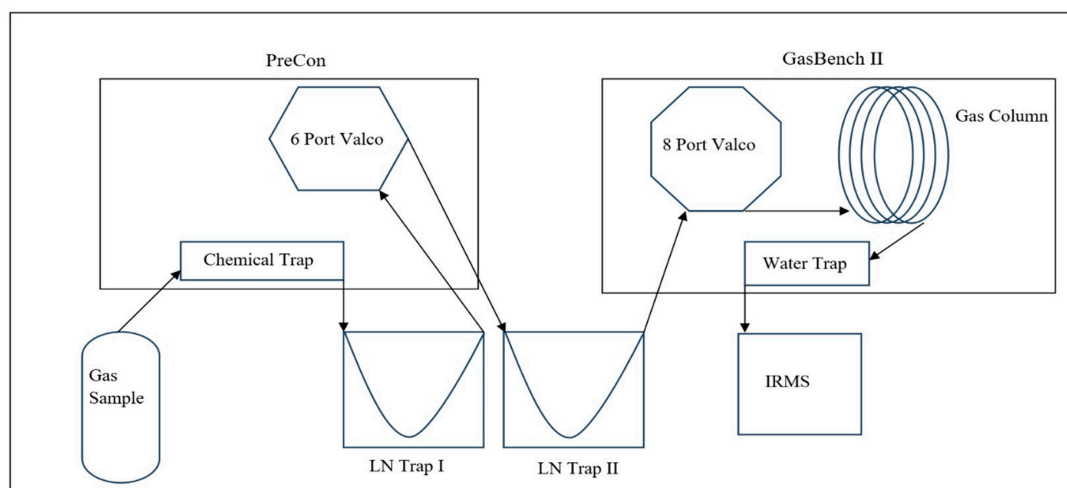


Figure 2. Schematic for the instrumentation of continuous flow measurements for nitrogen isotopes in gas.

The $^{15}\text{R}^\alpha$ and $^{15}\text{R}^\beta$ are the $^{15}\text{N}/^{14}\text{N}$ ratios at central (α) and terminal (β) nitrogen position in the linear N_2O molecule, respectively. $^{15}\text{R}_{\text{bulk}}$ denotes the average value of $^{15}\text{N}/^{14}\text{N}$ ratios. Standard is an international standard of atmospheric N_2 for N. The ^{15}N site preference was calculated from isotopomer ratios as $\text{SP} = \delta^{15}\text{N}^\alpha - \delta^{15}\text{N}^\beta$. The δ values and SP value are expressed in per mil (‰). The standard deviations of the measurements were 0.3‰ for $\delta^{15}\text{N}_{\text{bulk}}$ and 0.9‰ for $\delta^{15}\text{N}^\alpha$.

Conversion of measured ratios into isotopomers ratios was done using the following equations [12]

$$\begin{aligned} {}^{45}\text{R} &= {}^{15}\text{R}^\alpha + {}^{15}\text{R}^\beta + {}^{17}\text{R} \\ {}^{46}\text{R} &= {}^{18}\text{R} + ({}^{15}\text{R}^\alpha + {}^{15}\text{R}^\beta) {}^{17}\text{R} + {}^{15}\text{R}^\alpha {}^{15}\text{R}^\beta \\ {}^{31}\text{R} &= {}^{15}\text{R}^\alpha + {}^{17}\text{R} \\ {}^{32}\text{R} &= {}^{18}\text{R} + {}^{15}\text{R}^\alpha {}^{17}\text{R} \end{aligned}$$

Here ^{45}R and ^{46}R represent the isotopomers of N_2O that contribute to mass 45 and 46, ^{17}R represents the heavy oxygen and ^{31}R and ^{32}R correspond to isotopomers of NO .

3. Results and Discussion

3.1. N_2O Emissions Varying with Soil Chemistry

Soil properties of all the three positions at different depths are reported in Table 1. Our results for the C/N ratio show similarly low values among the three positions, ranging from 9% to 11%. Hence at our experimental site the variability of N_2O emissions must depend significantly on other factors such as water table depth and oxygen concentration, and not only on C/N ratio. Klemetsson et al. (2005) [36] have shown that at C/N ratios > 20 , N_2O emissions are low irrespective of other physical factors such as pH, water table, and soil oxygen content but when C/N ratios are low they affect N_2O emissions. Our results showed a negative trend N_2O emissions and bulk density. Leifeld (2018) [37] found similar results. Liu et al. (2019) [38] found a positive correlation between bulk density and N_2O emissions, which is in contradiction with our results. The concentrations of ammonium and nitrate increased from position A to C, without a trend with N_2O emissions. This indicated that inorganic nitrogen was not a driving factor responsible for the N_2O emissions. Organic matter content increased from position A to B and then decreased from position B to C, but due to similar C/N ratios, we expect it would not affect the N_2O emissions. No strong trends were observed between site preference and soil chemistry factors such as bulk density and C/N ratio. Also, according to the World Reference Base for Soil Resources (2007), soils containing 12% or more carbon are classified as peat. In our experimental site, all three positions had more than 12% of carbon and hence could be classified as peat [39].

Table 1. Soil properties at Kärevere field site. DM—dry matter.

Position and Depth	Bulk Density g/cm ³	DM %	pH _{KCl}	Organic Matter %	Total Carbon %	N %	NH ₄ -N mg/kg	NO ₃ -N mg/kg	C/N Ratio
A 0–10 cm	1.5	49.0	5.5	22.7	12.7	1.3	3.2	5.7	10.1
A 10–20 cm	1.8	59.1	5.9	15.8	8.8	0.9	1.9	16.0	9.9
A 20–30 cm	1.8	61.9	6.1	12.6	7.0	0.7	2.1	14.4	10.0
A 30–40 cm	2.0	71.7	6.4	7.7	4.3	0.4	1.2	11.4	10.7
B 0–10 cm	1.1	35.4	5.7	51.0	28.5	2.6	5.1	14.1	10.9
B 10–20 cm	1.1	35.3	6.1	51.9	29.0	2.8	5.5	15.0	10.5
B 20–30 cm	1.1	30.4	6.0	54.5	30.4	2.8	6.5	28.8	10.7
B 30–40 cm	1.1	30.2	6.2	55.8	31.2	2.9	10.1	35.1	10.6
B 40–50 cm	1.1	28.6	6.5	47.6	26.6	2.4	3.6	28.2	10.9
C 0–10 cm	1.4	44.1	5.2	30.1	16.8	1.5	5.5	20.6	11.0
C 10–20 cm	1.6	52.8	5.1	20.9	11.7	1.2	2.9	29.1	9.5
C 20–30 cm	1.8	59.8	5.0	12.3	6.9	0.7	2.6	11.6	9.5
C 30–40 cm	1.4	42.5	4.9	29.2	16.3	1.5	6.0	45.0	10.7
C 40–50 cm	1.7	51.4	5.1	15.4	8.6	0.8	2.8	19.5	11.0

3.2. N₂O Emissions Varying with Water Table

In response to changing water table depth, the N₂O emissions showed two maxima at water levels between −40 and −50 cm, and when the soil was submerged (Figure 3). Dobbie et al. (2001 and 2003) [9,40] have also observed similar trends in their experiment where they have shown an increase in N₂O emissions with increasing water-filled pore space (WFPS) [9,40,41]. Furthermore, Goldberg et al. (2009) [42] have observed that N₂O in fen peat is mostly produced at depths between 0.3 and 0.5 m. Also, it has been shown that the emissions peak at one optimum point and are at the lowest in dry or saturated soil [43,44]. This is similar to the soil-moisture optimum observed worldwide [7]. We also observed temporal variation of emissions from each position. High spatial and temporal variability of fluxes seems to be typical for N₂O and has been observed in both mineral and organic soils [7–9,27,30,37,38,40]. Characteristically large temporal variations of N₂O emissions have also reported in a review paper by Henault et al. (2012) [45].

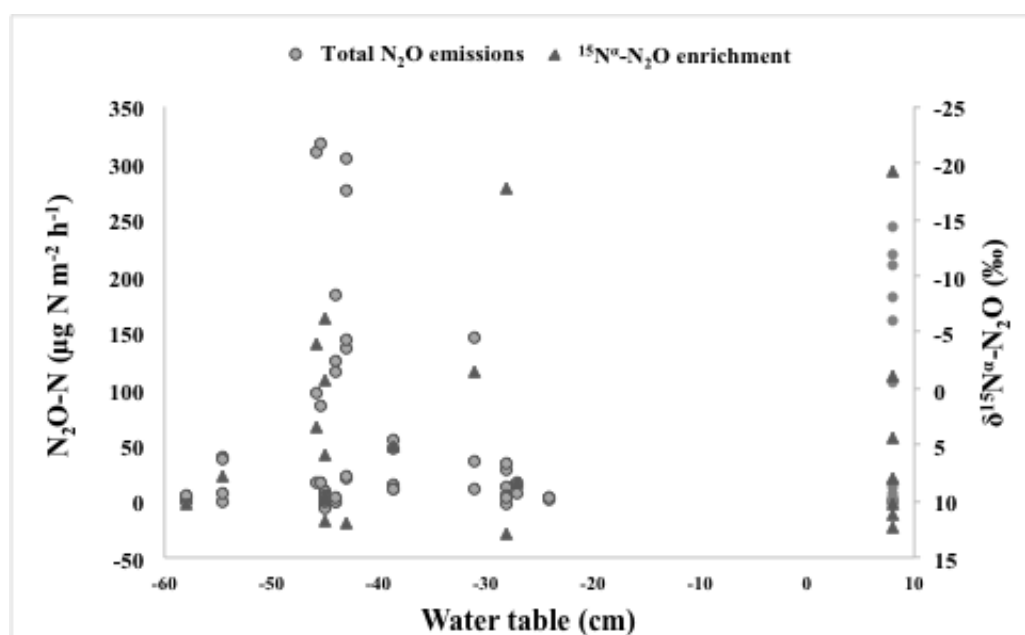


Figure 3. Total N₂O emissions and $\delta^{15}\text{N}^{\alpha}$ enrichment in N₂O versus water table. In flooded conditions, fluxes depend on O₂ concentration changing with flooding time. The parabolic trendline of N₂O emissions is shown ($R^2 = 0.08$; $p < 0.05$).

3.3. N_2O Emissions Varying with Flooding Time.

The N_2O emissions were observed to increase after the flooding over 80 minutes, after which a sudden drop was observed in N_2O emissions and emissions remained low at longer flooding times (Figure 4A). This also explains the high N_2O emissions observed during the positive water table as when the flooding process would begin, it would take some time to achieve anoxic conditions and during this time some N_2O bursts or peaks were observed. Hansen et al. (2014) [46] have observed a similar trend in agricultural soils where emissions increased after flooding until a maximum at a certain flooding time and after that decreased with a steep fall [46]. Similar trends have also been observed in rice paddies in Indonesia and China [47,48].

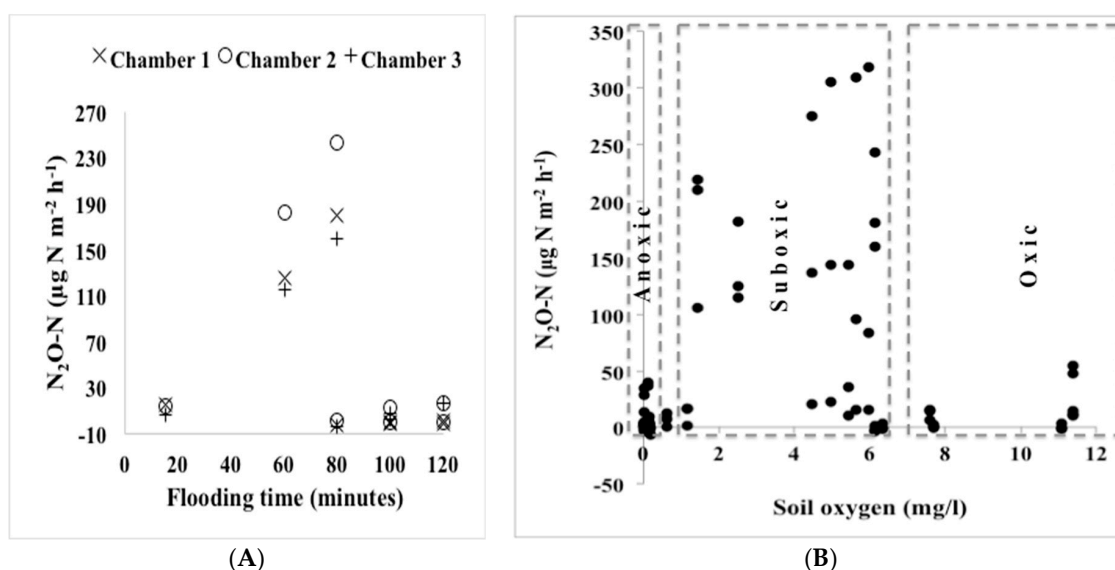


Figure 4. (A) N_2O emissions varying with flooding time from three chambers per session at Position C (see Figure 1). (B) Variation of N_2O emissions with varying oxygen content showing anoxic, suboxic, and oxic zones.

3.4. N_2O Emissions Varying with Oxygen Content

Under anoxic conditions (0 $\text{mg O}_2/\text{L}$), most of the N_2O emissions were low (Figure 4B). This could indicate reduction of N_2O to N_2 due to a lack of oxygen. From the suboxic peat (0.5–6 $\text{mg O}_2/\text{L}$) emissions were high and showed a peak at oxygen content of 6 mg/L . From the oxic peat (6–12 $\text{mg O}_2/\text{L}$), N_2O emissions were lower than from the suboxic peat but higher than from the anoxic peat. Vor et al. (2003) [40] and Rubol et al. (2012) [8] show similar trends in N_2O emissions where suboxic or intermediate oxygen content results in the highest N_2O emissions from the soil [10,49,50]. Furthermore, Zhua et al. (2013) [51] have also shown that as conditions approach an anoxic nature, heterotrophic denitrification is the major active process [51]. This coheres with our results and hypothesis and is further confirmed by the isotope results below.

3.5. Variation of Soil $\delta^{15}N_{\text{bulk soil}}$

The $\delta^{15}N$ values of total soil nitrogen showed low $\delta^{15}N$ (‰ air N_2) values with little variation with depth at position B, possibly due to its suboxic nature (Figure 5). However, in flooded position C there is a decreasing $\delta^{15}N_{\text{bulk soil}}$ trend with peat depth in the upper part of the section, which starts to increase again from the soil depth of 40 cm. This might be due to the flooding effect. In contrast, at position A, the $\delta^{15}N_{\text{soil}}$ values increased with soil depth to 30 cm, after which the $\delta^{15}N_{\text{soil}}$ decreased. The increasing trend of $\delta^{15}N_{\text{soil}}$ has also been observed by Brenner et al. (2001) [52] during their study in grasslands in California. They indicated soil inputs such as soil roots, as the cause for this trend [52]. However, as the flooding process was conducted for a time span of over a month, during which ten

sessions were conducted in our experiment, the microbial activity due to fluctuating water table depth and oxygen content could have been responsible for the enrichment of heavy nitrogen isotope during this time. Increased $\delta^{15}\text{N}$ values have also been observed in forest soil by Snider et al. (2009) [53].

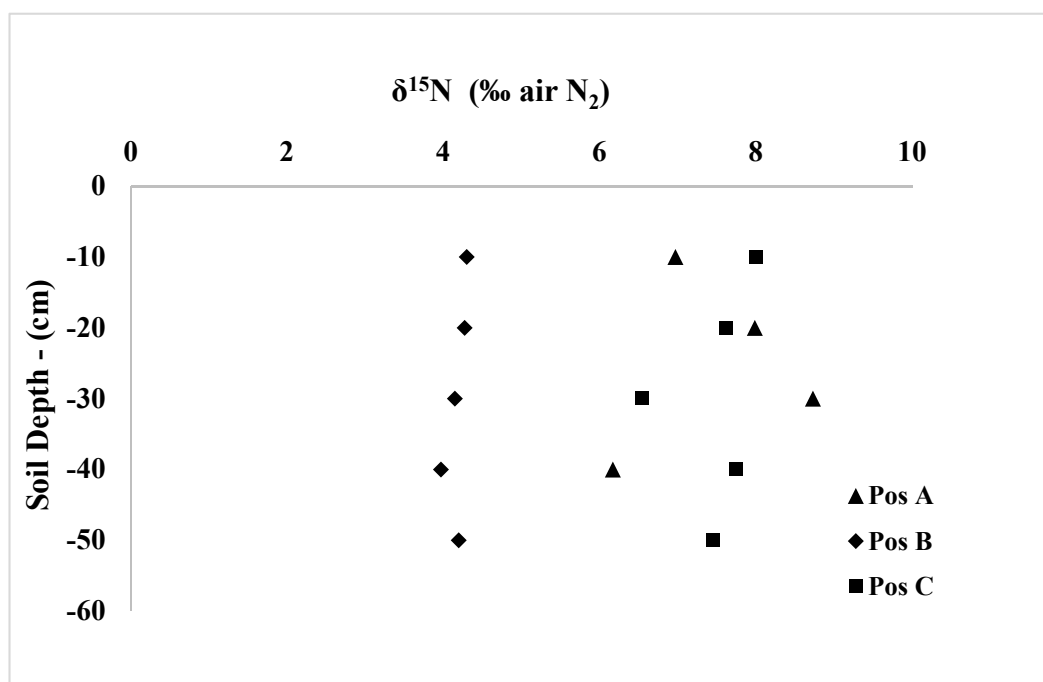


Figure 5. $\delta^{15}\text{N}$ ‰ values of the bulk soil varying with position and soil depth. Position (Pos) B has the lowest N_2O -N emission values (see Figure 4B).

3.6. $\delta^{15}\text{N}_{\text{gas}}$ and Site Preference in N_2O

Both total N_2O emissions and $\delta^{15}\text{N}$ values of the gas samples were highest at the water table depth of -40 to -50 cm (Figure 3). Schmidt et al. [16] have explained a decrease in heavy isotope at the central position of the N_2O molecule with increase of water table depth. The $^{15}\text{N}^\alpha$ enrichment trend in our data was similar to the total N_2O emissions showing an optimum around the -40 cm water table (Figure 3). The increasing enrichment (Figure 3) is in coherence with the results found by Sutka et al. [21] who observed an increase of $\delta^{15}\text{N}^\alpha$ produced by denitrifying bacteria with depletion of soil oxygen. SP values were negative (Figure 6A). This, with negligible N_2O emission (Figure 4B) and high soil ^{15}N abundance (Figure 5) indicated denitrification. In the suboxic peat the negative SP, high N_2O emissions and low soil ^{15}N abundance indicated incomplete denitrification.

Most of the earlier studies on N_2O site preference observed an increasing trend for site preference vs. N_2O oxygen isotopic composition [54–57] though no clear trend was observed between the oxygen isotope composition of N_2O and site preference under heterotrophic denitrification in pure bacterial cultures [21]. Interestingly in our suboxic peat (Pos B) site preference increased with $\delta^{18}\text{O}$ (Figure 6B). The positive relationship between site preference and $\delta^{18}\text{O}$ has been observed by a few studies focused on denitrification in soils [53,58]. Under the varying soil oxygen status, heavy oxygen enrichment was higher than heavy nitrogen enrichment, showing significant correlation (Figure 6C). This can be considered as one of the indicators of denitrification as the dominant producer of N_2O in the floodplain fen. Similar trends have been observed by Menyailo et al. (2006) [59] in their study of Siberian soils under denitrifying conditions. In our study, low values of site preference (SP; difference between the central and peripheral ^{15}N atoms) and $\delta^{18}\text{O}$ - N_2O in the captured gas samples indicate nitrifier denitrification in the floodplain fen (Figure 6B,C). This is also supported by the findings in relevant publications on N_2O production pathways [60–62].

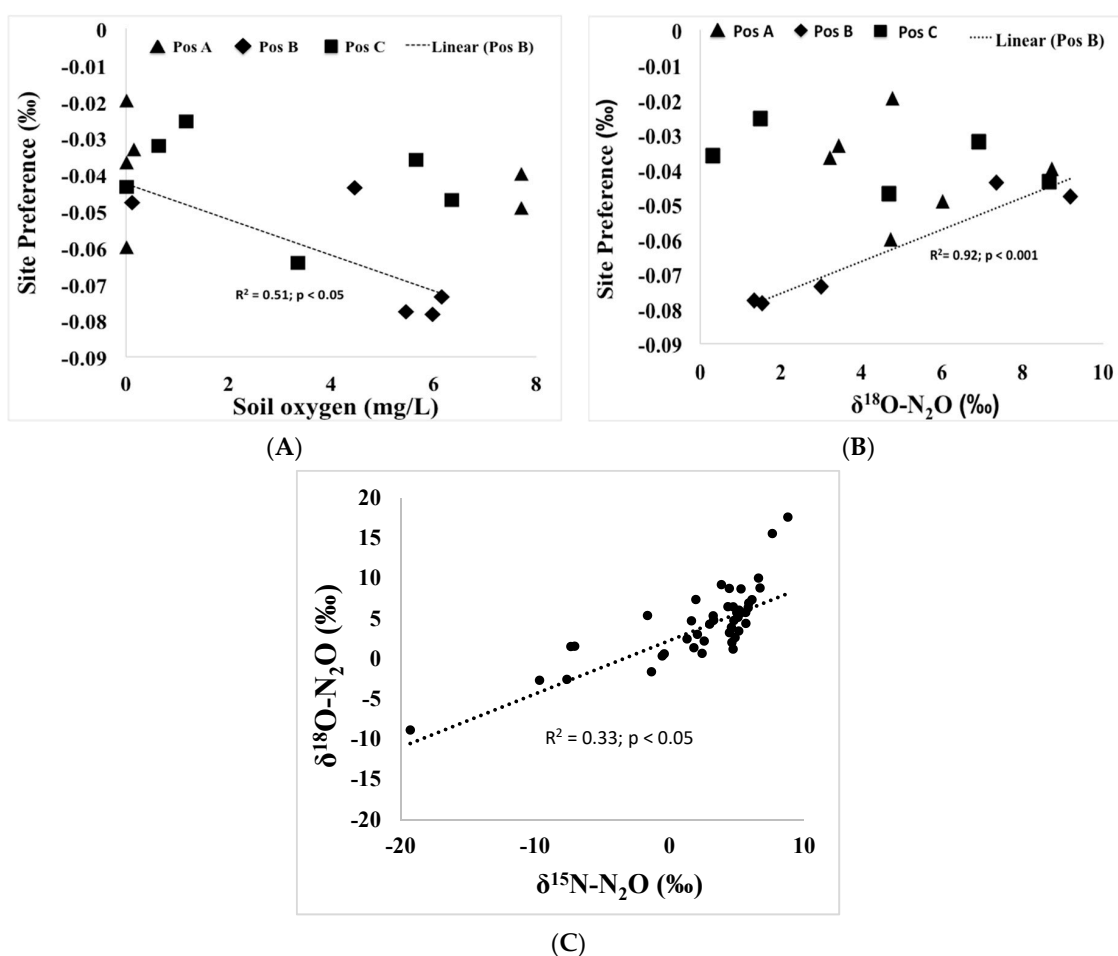


Figure 6. (A) Variation of site preference in gas samples in relationship with soil oxygen concentration. Position (Pos) A has anoxic conditions, Positions B and C are suboxic and oxic, respectively. (B) N_2O SP (site preference) vs. $\delta^{18}\text{O}$ relationship for all measurements. (C) N_2O isotopic signatures showing variation of $\delta^{18}\text{O}$ vs. $\delta^{15}\text{N}$.

Fluctuating water table in riparian zones [56] and floodplain fens [63] is a natural phenomenon that is increasing N_2O emissions. Agricultural use and climate change in floodplain fens will intensify N_2O losses and therefore, mitigation measures are necessary. Poyda et al. (2016) [64] propose to avoid arable use of floodplain fens. A productive three-cut system grassland would yield the lowest emission rate from high groundwater (long-term mean < 20 cm below the surface) [64]. For northern Europe, climate change models forecast increasing precipitation sum and more frequent climate events (floods and droughts; IPCC, 2014) [4], wherefore the range of water-table fluctuation will be most likely increasing in floodplains. Therefore, adaptation strategies and mitigation measures are becoming increasingly important. Using nuclear techniques will be helpful to understand processes and identify N_2O sources. That is necessary for the further development of mitigation measures [65].

4. Conclusions

In the anoxic floodplain fen peat, N_2O emission was low. Accumulation of the heavy nitrogen isotope in the soil, low values of site preference, and $\delta^{18}\text{O}-\text{N}_2\text{O}$ in the captured gas samples indicate nitrifier denitrification in the anoxic floodplain peat. In the suboxic peat the isotopic signals were similar but N_2O emissions were high, indicating that the denitrification was incomplete. Further investigation should focus on distinguishing N_2O production pathways using microbial analysis (metagenomic and qPCR approaches) and labelled ^{15}N techniques. This is important for better regulation of land use in floodplains to mitigate N_2O emissions.

Author Contributions: Conceptualisation: Ü.M., K.K. and J.P.; M.M., J.P. and Ü.M. conceived and designed the experiments; M.M. and J.P. performed the experiments; H.S. and M.M. performed the gas, water and soil analyses and analysed the data; M.M. and Ü.M. made visualisations; K.K. contributed materials and analysis tools; M.M. wrote the draft; K.K., J.P., Ü.M. and M.M. corrected and edited the paper. All authors have read and agreed to the published version of the manuscript.

Funding: The research was supported by the Ministry of Education and Research of Estonia (IUT2-16 and PRG-352 grants), the EU through European Regional Development Fund (ENVIRON and EcolChange Centres of Excellence, and the MOBTP101 returning researcher grant by Mobilitas⁺), and the Estonian Centre of Analytical Chemistry (AKKI). The methodological groundwork for the study was laid by IAEA's Coordinated Research Project (CRP) on "Strategic placement and area-wide evaluation of water conservation zones in agricultural catchments for biomass production, water quality and food security".

Conflicts of Interest: The authors declare no conflict of interest.

References

- Mander, Ü.; Tournebize, J.; Tonderski, K.; Verhoeven, J.T.A.; Mitsch, J.W. Planning and establishment principles for constructed wetlands and riparian buffer zones in agricultural catchments. *Ecol. Eng.* **2017**, *103*, 296–300. [[CrossRef](#)]
- Teiter, S.; Mander, Ü. Emission of N₂O, N₂, CH₄ and CO₂ from constructed wetlands for wastewater treatment and from riparian buffer zones. *Ecol. Eng.* **2005**, *25*, 528–541. [[CrossRef](#)]
- Verhoeven, J.T.A.; Arheimer, B.; Yin, C.G.; Hefting, M.M. Regional and global concerns over wetlands and water quality. *Trends Ecol. Evol.* **2006**, *21*, 96–103. [[CrossRef](#)] [[PubMed](#)]
- Stocker, T.F.; Qin, D.; Plattner, G.K.; Tignor, M.; Allen, S.K.; Boschung, J.; Nauels, A.; Xia, Y.; Bex, V.; Midgley, P.M. *Climate Change 2013: The Physical Science Basis*; Contribution of Working Group I to the Fifth Assessment Report of the Intergovernmental Panel on Climate Change; IPCC: Cambridge, UK; New York, NY, USA, 2013; pp. 1437–1446.
- Lu, Y.; Hongwen, X. Effects of Soil Temperature, Flooding, and Organic Matter addition on N₂O Emissions from a soil of Hongze Lake Wetland, China. *Sci. World J.* **2014**, *2014*, 272684. [[CrossRef](#)] [[PubMed](#)]
- Yano, M.; Toyoda, S.; Tokida, T.; Hayashi, K.; Hasegawa, T.; Makabe, A.; Yoshida, N. Isotopomer analysis of production, consumption and soil-to-atmosphere emission processes of N₂O at the beginning of paddy field irrigation. *Soil Biol. Biochem.* **2013**, *70*, 66–78. [[CrossRef](#)]
- Pärn, J.; Verhoeven, J.T.A.; Butterbach-Bahl, K.; Dise, N.B.; Ullah, S.; Aasa, A.; Egorov, S.; Espenberg, M.; Järveoja, J.; Jauhiainen, J.; et al. Nitrogen-rich organic soils under warm well-drained conditions are global nitrous oxide emission hotspots. *Nat. Commun.* **2018**, *9*, 1135. [[CrossRef](#)]
- Rubol, S.; Silver, W.L.; Bellin, A. Hydrologic control on redox and nitrogen dynamics in a peatland soil. *Sci. Total Environ.* **2012**, *432*, 37–46. [[CrossRef](#)]
- Dobbie, K.E.; Smith, K.A. The effects of temperature, water-filled pore space and land use on N₂O emissions from an imperfectly drained gleysol. *Eur. J. Soil Sci.* **2001**, *52*, 667–673. [[CrossRef](#)]
- Inubushi, K.; Furukawa, Y.; Hadi, A.; Purnomo, E.; Tsuruta, H. Seasonal changes of CO₂, CH₄ and N₂O fluxes in relation to land use change in tropical peatlands located in coastal area of South Kalimantan. *Chemosphere* **2003**, *52*, 603–608. [[CrossRef](#)]
- Toyoda, S.; Yano, M.; Nishimura, S.; Akiyama, H.; Hayakawa, A.; Koba, K.; Sudo, S.; Yagi, K.; Makabe, A.; Tobari, Y.; et al. Characterization and production and consumption processes of N₂O emitted from temperate agricultural soils determined via isotopomer ratio analysis. *Glob. Biogeochem. Cycles* **2011**, *25*, 1–17. [[CrossRef](#)]
- Toyoda, S.; Yoshida, N. Determination of Nitrogen Isotopomers of Nitrous Oxide on a Modified Isotope Ration Mass Spectrometer. *Anal. Chem.* **1999**, *71*, 4711–4718. [[CrossRef](#)]
- Yoshida, N.; Toyoda, S. Constraining the atmospheric N₂O budget from the intermolecular site preference in N₂O isotopomers. *Nature* **2000**, *405*, 330–334. [[CrossRef](#)] [[PubMed](#)]
- Yung, Y.L.; Miller, C.E. Isotopic fractionation of stratospheric nitrous oxide. *Science* **1997**, *278*, 1778–1780. [[CrossRef](#)] [[PubMed](#)]
- Popp, B.N.; Westley, M.B.; Toyoda, S.; Miwa, T.; John, E.D.; Yoshida, N.; Rust, T.M.; Sansone, F.J.; Russ, M.E.; Ostrom, N.E.; et al. Nitrogen and oxygen isotopomeric constraints on the origins and sea-to-air flux of N₂O in the oligotrophic subtropical North Pacific gyre. *Glob. Biogeochem. Cycles* **2002**, *16*, 1064. [[CrossRef](#)]

16. Schmidt, H.L.; Werner, R.A.; Yoshida, N.; Well, R. Is the isotopic composition of nitrous oxide an indicator for its origin from nitrification or denitrification? A Theoretical approach from referred data and microbiological and enzyme kinetic aspects. *Rapid Commun. Mass Spectrosc.* **2004**, *18*, 2036–2040. [CrossRef]
17. Well, R.; Flessa, H. Isotopologue signatures of N₂O produced by denitrification in soils. *J. Geophys. Res.* **2009**, *114*, 1–11. [CrossRef]
18. Yamulki, S.; Bol, R.; Wolf, I.; Grant, B.; Brumme, R.; Veldkamp, E.; Jarvis, S.C. Effects of dung and urine amendments on the isotopic content of N₂O released from grasslands. *Rapid Commun. Mass Spectrosc.* **2000**, *14*, 1356–1360. [CrossRef]
19. Perez, T.; Trumbore, S.E.; Tyler, S.C.; Matson, P.A.; Monasterio, O.; Rahn, T.; Griffith, D.W.T. Identifying the agricultural imprint on the global N₂O budget using stable isotopes. *J. Geophys. Res.* **2001**, *106*, 9869–9878. [CrossRef]
20. Sutka, R.L.; Ostrom, N.E.; Ostrom, P.H.; Gandhi, H.; Breznak, J.A. Nitrogen isotopomer site preference of N₂O produced by *Nitrosomonas europaea* and *Methylococcus capsulatus* bath. *Rapid Commun. Mass Spectrosc.* **2004**, *18*, 1411–1412. [CrossRef]
21. Sutka, R.L.; Ostrom, N.E.; Ostrom, P.H.; Breznak, J.A.; Gandhi, H.; Pitt, A.J.; Li, F. Distinguishing nitrous oxide production from nitrification and denitrification on basis of isotopomer abundances. *Appl. Environ. Microbiol.* **2005**, *72*, 638–644. [CrossRef]
22. Toyoda, S.; Motube, M.H.; Yamagishi, H.; Yoshida, N.; Tanji, Y. Fractionation of N₂O isotopomers during production by denitrifiers. *Soil Biol. Biochem.* **2005**, *37*, 1535–1545. [CrossRef]
23. Well, R.; Flessa, H.; Lu, X.; Ju, X.; Römheld, V. Isotopologue ratios of N₂O emitted from microcosms with NH₄ fertilizer arable soils under conditions favouring nitrification. *Soil Biol. Biochem.* **2008**, *40*, 2416–2426. [CrossRef]
24. Bol, R.; Toyoda, S.; Yamulki, S.; Hawkins, J.M.B.; Cardenas, L.M.; Yoshida, N. Dual isotope and isotopomer ratios of N₂O emitted from a temperate grassland soil after fertiliser application. *Rapid Commun. Mass Spectrom.* **2003**, *17*, 2550–2556. [CrossRef] [PubMed]
25. Well, R.; Kurganova, I.; de Gerenyu, V.L.; Flessa, H. Isotopomer signatures of soil emitted N₂O under different moisture conditions—A microcosm study with arable losses soil. *Soil Biol. Biochem.* **2006**, *38*, 2923–2933. [CrossRef]
26. Denk, T.R.A.; Mohn, J.; Decock, C.; Szczebak, D.L.; Harris, E.; Bahl, K.B.; Kiese, R.; Wolf, B. The nitrogen cycle: A review of isotope effects and isotope modelling approaches. *Soil Biol. Biochem.* **2017**, *105*, 121–137. [CrossRef]
27. Pérez, T.; Garcia-Montiel, D.; Trumbore, S.; Tyler, S.; de Camargo, P.; Moreira, M.; Piccolo, M.; Cerri, C. Nitrous oxide nitrification and denitrification ¹⁵N enrichment factors from amazon forest soils. *Ecol. Appl.* **2006**, *16*, 2153–2167. [CrossRef]
28. Cardena, L.M.; Chadwick, D.; Scholefield, D.; Fychan, R.; Marley, C.L.; Jones, R.; Bol, R.; Well, R.; Vallejo, A. The effect of diet manipulation on nitrous oxide and methane emissions from manure application to incubated grassland soils. *Atmos. Environ.* **2007**, *33*, 7096–7107. [CrossRef]
29. Rückauf, U.; Augustin, J.; Russow, R.; Merbach, W. Nitrate removal from drained and reflooded fen soils affected by soil N transformation processes and plant uptake. *Soil Biol. Biochem.* **2004**, *36*, 77–90. [CrossRef]
30. Tauchnitz, N.; Spott, O.; Russow, R.; Bernsdorf, S.; Glaser, B.; Meissner, R. Release of nitrous oxide and dinitrogen from a transition bog under drained and rewetted conditions due to denitrification: Results from a ¹⁵N-nitrate–bromide double-tracer study. *Isot. Environ. Health Stud.* **2015**, *51*, 300–321. [CrossRef]
31. Yang, W.H.; Teh, Y.A.; Silver, W.L. A test of a field-based ¹⁵N–nitrous oxide pool dilution technique to measure gross N₂O production in soil. *Glob. Chang. Biol.* **2011**, *17*, 3577–3588. [CrossRef]
32. FAO Organization. Physical Properties|FAO Soils Portal|Food and Agriculture Organization of the United Nations. 2020. Available online: <http://www.fao.org/soils-portal/soil-survey/soil-properties/physical-properties/en/> (accessed on 21 January 2020).
33. Silc, T.; Stanek, W. Bulk density estimation of several peats in northern Ontario using the von post humification scale. *Can. J. Soil Sci.* **1977**, *57*, 75. [CrossRef]
34. Hyodo, A.; Malghani, S.; Zhou, Y.; Mushinski, R.M.; Toyoda, S.; Yoshida, N.; Boutton, T.W.; West, J.B. Biochar and amendment suppresses N₂O emissions but has no impact on ¹⁵N site preference in an anaerobic soil. *Rapid Commun. Mass Spectrosc.* **2018**, *33*, 165–175. [CrossRef] [PubMed]

35. Potter, K.E.; Ono, S.O.; Prinn, R.G. Fully automated, high-precision instrumentation for the isotopic analysis of tropospheric N₂O using continuous flow isotope ratio mass spectrometry. *Rapid Commun. Mass Spectrom.* **2013**, *27*, 1723–1738. [[CrossRef](#)] [[PubMed](#)]
36. Klemedtsson, L.; Arnold, V.; Weslien, K.; Gundersen, P. Soil C/N ratio as a scalar parameter to predict nitrous oxide emissions. *Glob. Chang. Biol.* **2005**, *11*, 1142–1147. [[CrossRef](#)]
37. Leifeld, J. Distribution of nitrous oxide emissions from managed organic soils under different land uses estimated by the peat C/N ratio to improve national GHG inventories. *Sci. Total Environ.* **2018**, *631*, 23–26. [[CrossRef](#)]
38. Liu, H.; Zak, D.; Rezanezhad, F.; Lennartz, B. Soil degradation determines release of nitrous oxide and dissolved organic carbon from peatlands. *Environ. Res. Lett.* **2019**, *14*, 094009. [[CrossRef](#)]
39. FAO. *World Reference Base for Soil Resources*; FAO: Rome, Italy, 2007.
40. Dobbie, K.E.; Smith, K.A. Nitrous oxide emission factors for agricultural soils in Great Britain: Then impact of soil water filled pore space and other controlling variables. *Glob. Chang. Biol.* **2003**, *9*, 204–218. [[CrossRef](#)]
41. Dobbie, K.E.; Smith, K.A. The effect of water table depth on emissions of N₂O from grassland soil. *Soil Use Manag.* **2006**, *22*, 22–28. [[CrossRef](#)]
42. Goldberg, S.D.; Knorr, K.H.; Blodau, C.; Lischeid, G.; Gebauer, G. Impact of altering the water table height of an acidic fen on N₂O and NO fluxes and soil concentrations. *Glob. Chang. Biol.* **2009**, *16*, 220–223. [[CrossRef](#)]
43. Schauffler, G.; Kitzler, B.; Schindlbacher, A.; Skiba, U.; Sutton, A.; Zechmeister-Boltenstern, S. Greenhouse gas emissions from European soils under different land use: Effects of Soil Moisture and Temperature. *Eur. J. Soil Sci.* **2010**, *61*, 683–696. [[CrossRef](#)]
44. Berglund, Ö.; Berglund, K. Influence of water table and soil properties on emissions of greenhouse gases from cultivated peat soil. *Soil Biol. Biochem.* **2011**, *43*, 923–931. [[CrossRef](#)]
45. Henault, C.; Grossel, A.; Mary, B.; Roussel, M.; Leonard, J. Nitrous oxide emission by agricultural soils: A review of spatial and temporal variability for mitigation. *Pedosphere* **2012**, *22*, 426–433. [[CrossRef](#)]
46. Hansen, M.; Clough, T.J.; Elberling, B. Flooding-induced N₂O emissions bursts controlled by pH and nitrite in agricultural soils. *Soil Biol. Biochem.* **2014**, *69*, 17–24. [[CrossRef](#)]
47. Xing, G.X.; Shi, S.L.; Shen, G.Y.; Du, L.J.; Xiong, Z.Q. Nitrous oxide emissions from paddy soil in three rice based cropping systems in China. *Nutr. Cycl. Agroecosyst.* **2002**, *64*, 135–143. [[CrossRef](#)]
48. Purwanto, B.H.; Sari, N.N.; Utami, S.N.H.; Hanudin, E.; Sunarminto, B.H. Effect of flooding duration on nitrous oxide emissions from organic and conventional rice cultivation system in Central Java, Indonesia. *IOP Conf. Ser. Earth Environ. Sci.* **2018**, *215*, 1–6. [[CrossRef](#)]
49. Vor, T.; Dyckmans, J.; Loftfield, N.; Beese, F.; Flessa, H. Aeration effects on CO₂, N₂O and CH₄ emission and leachate composition of a forest soil. *J. Plant Nutr. Soil Sci.* **2003**, *166*, 39–46. [[CrossRef](#)]
50. Bollman, A.; Conrad, R. Influence of O₂ availability on NO and N₂O release by nitrification and denitrification in soils. *Glob. Chang. Biol.* **1998**, *4*, 387–396. [[CrossRef](#)]
51. Zhua, X.; Burger, M.; Doane, T.A.; Horwath, W.R. Ammonia oxidation pathways and nitrifier denitrification are significant sources of N₂O and NO under low oxygen availability. *Proc. Natl. Acad. Sci. USA* **2013**, *110*, 6328–6333. [[CrossRef](#)]
52. Brenner, D.L.; Amundson, R.; Baisden, W.T.; Kendall, C.; Harden, J. Soil N and ¹⁵N variation with time in a California annual grassland ecosystem. *Geochim. Cosmochim. Acta* **2001**, *65*, 4171–4186. [[CrossRef](#)]
53. Snider, D.M.; Schiff, S.L.; Spoelstra, J. ¹⁵N/¹⁴N and ¹⁸O/¹⁶O stable isotope ratios of nitrous oxide produced during denitrification in temperate forest soils. *Geochim. Cosmochim. Acta* **2009**, *73*, 877–888. [[CrossRef](#)]
54. Köster, J.R.; Well, R.; Dittert, K.; Giesemann, A.; Lewicka-Szczebak, D.; Mühling, K.H.; Herrmann, A.; Lammel, J.; Senbayram, M. Soil denitrification potential and its influence on N₂O reduction and N₂O isotopomer ratios. *Rapid Commun. Mass Spectrosc.* **2013**, *27*, 2363–2373.
55. Mothet, A.; Sebilo, M.; Laverman, A.M.; Vauy, V.; Mariotti, M. Is site preference of N₂O a tool to identify benthic denitrifier N₂O. *Environ. Chem.* **2013**, *10*, 281–284. [[CrossRef](#)]
56. Mander, Ü.; Well, R.; Weymann, D.; Soosar, K.; Maddison, M.; Kanal, A.; Löhmus, K.; Truu, J.; Augustin, J.; Tournebize, J. Isotopologue ratios of N₂O and N₂ measurements underpin the importance of denitrification in differently N-loaded riparian alder forests. *Environ. Sci. Technol.* **2014**, *48*, 11910–11918. [[CrossRef](#)] [[PubMed](#)]
57. Lewicka-Szczebak, D.; Augustin, J.; Giesemann, A.; Well, R. Quantifying N₂O reduction to N₂ based on N₂O isotopocules validation with independent methods. *Biogeosciences* **2017**, *14*, 711–732. [[CrossRef](#)]

58. Ostrom, N.E.; Pitt, A.; Sutka, R.; Ostrom, P.H.; Grandy, A.S.; Huizinga, K.M.; Robertson, G.P. Isotopologue effects during N₂O reduction in soils and in pure cultures of denitrifiers. *J. Geophys. Res.* **2007**, *112*, 1–12. [[CrossRef](#)]
59. Menyailo, O.V.; Hungate, B.A. Stable isotope discrimination during soil denitrification: Production and consumption of nitrous oxide. *Glob. Biogeochem. Cycles* **2006**, *20*, 1–10. [[CrossRef](#)]
60. Butterbach-Bahl, K.; Baggs, E.M.; Dannenmann, M.; Kiese, R.; Zechmeister-Boltenstern, S. Nitrous oxide emissions from soils: How well do we understand the processes and their controls? *Philos. Trans. R. Soc. B Biol. Sci.* **2013**, *368*, 20130122. [[CrossRef](#)]
61. Hu, H.W.; Chen, D.; He, J.Z. Microbial regulation of terrestrial nitrous oxide formation: Understanding the biological pathways for prediction of emission rates. *FEMS Microbiol. Rev.* **2015**, *39*, 729–749. [[CrossRef](#)]
62. Wrage-Mönnig, N.; Horn, M.A.; Well, R.; Müller, C.; Velthof, G.; Oenema, O. The role of nitrifier denitrification in the production of nitrous oxide revisited. *Soil Biol. Biochem.* **2018**, *123*, A3–A16. [[CrossRef](#)]
63. Tiemeyer, B.; Borraz, E.A.; Augustin, J.; Bechtold, M.; Beetz, S.; Beyer, C.; Drösler, M.; Ebli, M.; Eickenscheidt, T.; Fiedler, S.; et al. High emissions of greenhouse gases from grasslands on peat and other organic soils. *Glob. Chang. Biol.* **2016**, *22*, 4134–4149. [[CrossRef](#)]
64. Poyda, A.; Reinsch, T.; Kluss, C.; Loges, R.; Taube, F. Greenhouse gas emissions from fen soils used for forage production in northern Germany. *Biogeosciences* **2016**, *13*, 5221–5244. [[CrossRef](#)]
65. Zaman, M.; Müller, C.; Sanz-Cobena, A.; Kim, D.G.; Ding, W.; Borzouei, A.; Dawar, K.; Urquiaga, S.; Heng, L.K. The role of nuclear techniques in developing mitigation options for agricultural derived greenhouse gases. *Geophys. Res. Abstr.* **2018**, *20*, 15355.



© 2020 by the authors. Licensee MDPI, Basel, Switzerland. This article is an open access article distributed under the terms and conditions of the Creative Commons Attribution (CC BY) license (<http://creativecommons.org/licenses/by/4.0/>).